

Semiclassical wave packet tunneling in real-time

Joachim Ankerhold* and Markus Saltzer

Physikalisches Institut, Albert-Ludwigs-Universität Freiburg,

Hermann-Herder-Straße 3, D-79104 Freiburg, Germany

(Dated: November 3, 2018)

Abstract

Quantum mechanical real-time tunneling through general scattering potentials is studied in the semiclassical limit. It is shown that the exact path integral of the real-time propagator is dominated in the long time sector by quasi-stationary fluctuations associated with caustics. This leads to an extended semiclassical propagation scheme for wave packet dynamics which accurately describes deep tunneling through static and, for the first time, driven barrier potentials.

PACS numbers: 03.65.Sq,31.15.Kb,73.40.Gk,05.45.Mt

arXiv:quant-ph/0210135v1 18 Oct 2002

*Electronic address: ankerhold@physik.uni-freiburg.de

I. INTRODUCTION

Tunneling through a potential barrier is one of the most fascinating aspects of quantum mechanics. In recent years a particular challenge has been to understand tunneling in complex systems using semiclassical methods. However, any simple description is seemingly hampered by the fact that a quantum mechanical object running towards a barrier with a typical energy smaller than the barrier height may penetrate it even though all classical trajectories with such energies are reflected completely. Thus, for static observables like e.g. tunnel splittings one works in the *energy domain* and calculates the energy dependent Green's function semiclassically by switching from a real-time orbit outside the barrier to an orbit in imaginary time, i.e. with imaginary momentum, under the barrier. This technique can be traced back to the "old" WKB approximation [1] and meanwhile has been successfully extended to extract e.g. tunnel splittings also for systems with classically chaotic dynamics [2]. The crucial question is then: Can semiclassical tunneling also be described in the *real-time domain*? This issue has turned into a fundamental challenge for our understanding of semiclassics in general and systems with explicit time dependence as e.g. in the context of driven tunneling and control of tunneling [3] or tunneling in the presence of chaos [4] in particular.

The probability amplitude for a particle initially at q_i to be at q_f after time t is given by Feynman's path integral representation of the propagator as [5]

$$G(q_f, q_i, t) \equiv \langle q_f | e^{-iHt/\hbar} | q_i \rangle = \int \mathcal{D}[q] e^{iS[q]/\hbar}. \quad (1)$$

The integral sums over all paths running from q_i to q_f in time t where each contribution is weighted according to its action $S[q] = \int_{q_i}^{q_f} dq \sqrt{2m[E - V(q)]} - Et$ with potential $V(q)$ and energy $E = E(q_f, q_i, t)$. Due to the oscillating integrand in (1) tunneling appears to be the result of a complex interference pattern. In the semiclassical limit the path sum is dominated by the contributions of the stationary paths $\delta S[q_{cl}] = 0$ obeying Newton's equation of motion and small fluctuations around them. In the last decade efficient semiclassical propagation schemes based on Gaussian wave packets have been developed, certainly the most powerful known as the Hermann-Kluk propagator (HK) [6]. However, the inclusion of deep tunneling (may be even in presence of external driving) has not been satisfactory yet. In fact, it was found that classically allowed real-time trajectories running *over* the barrier are not sufficient to capture strong tunneling [7, 8]. Various extensions have thus been attempted.

By propagating a large number of initial wave packets tunnel splittings in a double well potential could be extracted, however, in single wave packet motion tunneling effects were absent [9]. As for barrier penetration no low energy stationary orbit exists along the real axis, it is tempting to think that one may find one in the complex plane [8]. An individual path circumventing—in real-time—the barrier region in a complex coordinate plane is assumed, but its existence is still elusive. In [10] orbits run along the real axis, but the semiclassical propagation over the time interval t is time sliced into steps over intermediate intervals. This spawning of orbits turns out to be numerically extremely expensive already for two slices and improves tunneling amplitudes only for energies not too far below the barrier top.

In the sequel we re-examine the semiclassical barrier penetration through scattering potentials starting from the exact expression (1). Our idea is this: While in the energy domain tunneling is described within a complex time plane, here, we study classical mechanics for complex energies. Our analysis reveals how tunneling is encoded in the quantum propagator (1) in terms of real-time orbits. In particular, it turns out that an individual complex “tunneling path” does not exist. Based on these results we extend the conventional HK to semiclassical wave packet dynamics in the deep tunneling regime not only through static potentials, but, for the first time, report also on accurate results for driven tunneling. The approach is shown to be very efficient for one-dimensional systems and may thus serve as a promising starting point for higher dimensional studies.

II. COMPLEX MECHANICS AND SEMICLASSICAL APPROXIMATION

We consider the motion of a particle of mass $m = 1$ in a general one-dimensional, symmetric barrier potential $V(q)$ where the barrier top is located at $q = 0$ with $V(0) = V_0$. $V(q)$ is assumed to be a smooth and analytic function of q that can be approximated around $q = 0$ by an inverted harmonic oscillator and for large $|q|$ falls off as $V(q) \rightarrow V_0/[q/l]^{2k}$, $k \geq 2$, integer, with a typical barrier length scale l . A sufficiently high barrier is taken for granted. Typical examples include $V_k(q) = V_0/[1 + (q/l)^2]^k$, but our results also apply to the Eckart barrier $V_0/\cosh(q/l)^2$ and the Gaussian barrier $V_0 \exp(-q^2/l^2)$.

Now, think of a wave packet $\psi(q_i, 0)$ localized to the far right ($q_i > 0$) which is propagated towards the barrier according to $\psi(q_f, t) = \int dq_i G(q_f, q_i, t) \psi(q_i, 0)$. We are interested in that portion of the packet that after time t arrives on the far left ($q_f = -q_i < 0$). All real orbits

connecting the two asymptotic regions run over the barrier ($E > V_0$) and as, for fixed endpoints, t becomes large they spend most of their time in the parabolic range around $q = 0$. There, the marginal stability of trajectories causes the semiclassical $G(-q_i, q_i, t)$ to die out exponentially in contrast to exact results [7]. Classical orbits with $E < V_0$ coming from the far right or left reach the right or left flank of the barrier at turning points (TPs) q_0 and $-q_0$, respectively; the long time properties of the path integral (1) are therefore governed by the dynamics in the “forbidden” range between the TPs. Mathematically, for $E < V_0$ no *real* stationary phase point to (1) obeying the proper boundary conditions exists in function space. The usual procedure is then an analytic continuation meaning here to extend classical mechanics to the complex coordinate plane.

Newton’s equation of motion, $\ddot{q} + V'(q) = 0$, where $\dot{q} = dq/dt$ and $V' = dV/dq$, translates for complex $q = x + iy$ into

$$\ddot{x} + r_x = 0, \quad \ddot{y} + j_x = 0. \quad (2)$$

Here, $V(q) = r(x, y) + ij(x, y)$ and the subscript x [y] denotes the partial derivative with respect to x [y]. We further exploited that for analytic functions $V(q)$ Cauchy’s relations $r_x = j_y$ and $r_y = -j_x$ apply. From (2) one simply finds that the total energy $E = \epsilon_{\text{re}} + i\epsilon_{\text{im}}$ and its real and imaginary parts

$$\epsilon_{\text{re}} = (\dot{x}^2 - \dot{y}^2)/2 + r(x, y) \quad \text{and} \quad \epsilon_{\text{im}} = \dot{x}\dot{y} + j(x, y), \quad (3)$$

respectively, are constants of motion. How does the corresponding classical mechanics look like? For low energies the TPs $q_0, -q_0$ lie in the range where $V(q)$ can be approximated by its asymptotic behavior. Hence, we consider paths starting from large $q_i = x_i > 0$ along the real axis with complex momentum $p_i \equiv \dot{q}_i = \dot{x}_i + i\dot{y}_i$. Typical trajectories are depicted in fig. 1. While basically three kinds of orbits can be distinguished, the common behavior is that as the barrier vanishes asymptotically, for large distances from the top the classical motion tends to be a free motion. If we represent trajectories in the form $q(t) = R(t)e^{i\phi(t)}$, for very large R they run close to straight lines with constant $\phi(q_i, p_i)$ depending merely on the initial phase space variables. Let us now discuss the types of orbits in detail.

First, we look at class (a) as it is the only one where orbits cross the line $x = 0$ ($\phi = \pi/2$) to reach the other side of the barrier. For such orbits we need initially $\dot{x}_i < 0$ (otherwise they would run away from the barrier anyway) and for the discussion assume $\dot{y}_i > 0$ implying $\epsilon_{\text{im}} = \dot{x}_i\dot{y}_i < 0$, see Eq. (3). We further note the asymptotic form of $V(q) = r(q) + ij(q)$

using polar coordinates:

$$r(R, \phi) = \frac{\cos(2k\phi)}{(R/l)^{2k}}, \quad j(R, \phi) = -\frac{\sin(2k\phi)}{(R/l)^{2k}}. \quad (4)$$

One sees immediately that a successful crossing of the dividing surface must happen with $\dot{y} > 0$ (and $\dot{x} < 0$ of course). Namely, at $\phi = \pi/2$ the imaginary part j vanishes so that $\epsilon_{\text{im}} = \dot{x}\dot{y} = \dot{x}_i\dot{y}_i < 0$ meaning $\dot{y} > 0$. For the required energy one derives $|\epsilon_{\text{im}}| > r(x_i, 0) = V(x_i)$. Starting, however, from the imaginary axis with $\dot{x} < 0$ and $\dot{y} > 0$, i.e. in the direction of decreasing $|V(q)|$, always generates an orbit reaching the asymptotic left side of the barrier far from the real axis ($\phi < \pi$). We conclude that a simple “tunneling path” connecting the asymptotic segments of the real axis on either side of the barrier via a tour through the complex plane does not exist. This is in sharp contrast to tunneling for fixed energy. There, the energy dependent Greens function $K(q_f, q_i, E)$ exhibits stationary phase points in imaginary time corresponding to classical paths running with energy E in the inverted potential through the barrier range from q_i to q_f . Here, for real-time tunneling a stationary phase path to the quantum propagator $G(q_f, q_i, t)$ even with complex energy cannot be found. This important result may also reflect the quite different roles “energy” and “time” play in quantum mechanics.

For our analysis the consequences are two-fold: on the one hand complex trajectories in class (a) do not play any role for a semiclassical approximation to $G(q_f, q_i, t)$, and on the other hand the path integral in (1) is in the low energy sector completely determined by fluctuations. To find its dominant contributions thus means to detect the dominant fluctuations; these are points in function space which lie close to orbits with $\delta S[q] = 0$ and also obey the proper boundary conditions. Accordingly, we consider the remaining two classes of paths.

The second class (b) contains orbits with small but non-vanishing energies $0 < |\epsilon_{\text{im}}| < r(x_i, 0)$ which may exhibit TPs in the complex plane and always live on the same side of the barrier. Hence they are not relevant either. In the third class (c) trajectories have real total energy E , i.e. $\epsilon_{\text{im}} = 0$, but start with purely imaginary momenta $\dot{x}_i = 0$ and, as assumed, small $\epsilon_{\text{re}} = -\dot{y}_i^2/2 + r(x_i, 0)$. These orbits display crucial features as we will explain in the following. For that purpose we focus on the limit $\epsilon_{\text{re}} = 0$ and follow paths with $x_i > 0, \dot{y}_i > 0$. Writing asymptotically $q(t) = R(t)e^{i\phi}$ one obtains

$$\phi(x_i, \dot{y}_i) \equiv \phi_c^+ = \pi/[2(k+1)]. \quad (5)$$

Hence, after a transient period of time *all* those orbits run along the *same* line in the complex plane independent of their starting points x_i . And since they carry the same energy, they are also focused in phase space so that the line ϕ_c defines a caustic. Were the trajectories optical rays, $\phi = \phi_c^+$ would be a burning line. Due to symmetry the same holds true for the complementary line $-\phi_c^+$ and the lines $\pi \pm \phi_c^+$ on the other side of the barrier. Typically, a caustic is associated with unstable orbits and fluctuations connecting them which renders a simple Gaussian semiclassics insufficient [5]. To verify this scenario here, we consider small deviations $\delta q = \delta x + i\delta y$ around a certain orbit $\bar{q}(x_i; t)$. By linearizing the equations of motion (2) one gains $(\delta\dot{x}, \delta\dot{y})^T = \mathbf{M} (\delta x, \delta y)^T$ where \mathbf{M} is the stability matrix evaluated along $\bar{q}(t)$. Along $\phi = \phi_c^+$ its diagonal elements are $-\bar{r}_{xx} > 0$ and the off-diagonal elements vanish $\bar{j}_{xx} = 0$. Accordingly, all trajectories merging along the burning lines are unstable. Small deviations in phase space can lead from an orbit $\bar{q}(x_i; t)$ to another one $\bar{q}(x'_i; t)$ and even allow for a turn from positive to negative momentum to run along the $\bar{q}(x'_i; t)$ -orbit back towards the real axis. As asymptotically paths creep along ϕ_c^+ , jumps from very small positive to negative momenta require only tiny fluctuations. The reversed orbit crosses the real axis at x'_i and approaches the complementary burning line $-\phi_c^+$ in the lower halfplane. There, a similar kind of deviation drives it to still another $\bar{q}(x''_i; t)$ to reach again ϕ_c^+ and so forth and back. By subsequently running through these cycles between the caustics at $\pm\phi_c^+$ a net-motion into the direction of the barrier top may be generated. On the left side of the barrier ($x_i < 0$) the same kind of scenario exists and at the top $x = 0$ the burning lines intersect (depending in detail on $V(q)$ within $|q/l| \lesssim 1$, see fig 1.) so that small deviations in the vicinity of the bottleneck $x = 0$ may lead from the set of right-barrier paths to that of left-barrier paths and vice versa. This allows for a motion starting in $x_i > 0$ to eventually reach the range on the opposite side of the barrier. So far the above discussion is restricted to class (c)-orbits with $\epsilon_{re} = 0$. However, for finite but small ϵ_{re} orbits merge close to the burning lines, and we find basically the same situation. The conclusion is that two real axis paths with TPs at q_0 and $-q_0$, respectively, are linked by a sequence of real-time complex plane orbits tied together by small fluctuations near caustic lines. Since this under-barrier-motion is not a purely stationary one obeying (2), but can be seen as nearly stationary as it follows classical orbits most of the time, it describes quasi-stationary fluctuations (QSF). The QSF allow to move from $q_i > 0$ through the barrier range towards $q_f < 0$ and this way dominate in absence of true stationary points, $\delta S[q] = 0$ with $q(0) = q_i, q(t) = q_f$, the path

integration in $G(q_f, q_i, t)$ between the TPs.

III. EXTENDED SEMICLASSICAL PROPAGATOR

The action of the QSF can simply be approximated. For a cycle from x_i with $\bar{q}(x_i; t)$ to $x'_i < x_i$ with $\bar{q}(x'_i; t)$ in the interval δt we find with Cauchy's formula $S(x'_i, x_i, \delta t) \approx i|W(x'_i, x_i)| - E\delta t$ where the short action is $W(x', x) = \int_{x'}^x dq \sqrt{2m[E - V(q)]}$ and the portion from the phase space deviation along ϕ_c^+ is negligible. Accordingly, $S(-q_0, q_0, \Delta t) \approx i|W(-q_0, q_0)| - E\Delta t$ where Δt is the time interval spent between the real axis TPs $q_0, -q_0$. Hence, one arrives at the crucial result that the real-time motion of the QSF gives rise to an imaginary part in the action which is identical to the known instanton or WKB exponent. The full action for a low energy motion from $q_i > 0$ to $-q_i$ now consists of two classical real axis segments from q_i to q_0 and from $-q_0$ to $-q_i$, respectively, and QSF inbetween, i.e. $S(-q_i, q_i, t) \approx 2W(q_0, q_i) + i|W(-q_0, q_0)| - Et$. In the semiclassical $G(-q_i, q_i, t)$ the exponential of this action is accompanied by the contribution of Gaussian fluctuations around the real axis segments.

The most powerful representation of the semiclassical propagator is the so-called Hermann-Kluk propagator (HK) [6]. It has the advantage of being determined by an initial value problem for the classical trajectories, namely,

$$G_{\text{HK}}(q_f, q_i, t) = \int \frac{dqdp}{2\pi\hbar} h(q_f, q_i, t, p, q) R(p, q, t) e^{iS(p, q, t)/\hbar} \quad (6)$$

with the fluctuation prefactor $R(p, q, t)$ and an overlap factor $h(q_f, q_i, t, p, q) = \langle q_f | \gamma(p, q, t) \rangle \langle \gamma(p, q) | q_i \rangle$ where

$$\langle x | \gamma(p, q, t) \rangle = \left(\frac{\gamma}{\pi} \right)^{1/4} \exp \left\{ -\frac{\gamma}{2} [x - q(t)]^2 + \frac{i}{\hbar} p(t) [x - q(t)] \right\} \quad (7)$$

is a Gaussian wave packet centered around the phase space point $\{p(t), q(t)\}$. In (6) one runs in the time interval t real trajectories from $\{p, q\}$ to $\{p(t), q(t)\}$ where the contribution of each orbit is weighted according to its action and fluctuation prefactor and the Gaussian overlap of its end-points with those of the propagator.

The usual HK (6) is exact for a pure parabolic barrier and therefore captures tunneling only for harmonic fluctuations around the barrier top but fails for long times [8]. To overcome this drawback we apply the results developed above and formally split the propagator in

phase space: $G(q_f, q_i, t) = G_>(q_f, q_i, t) + G_<(q_f, q_i, t)$ where $G_>$ [$G_<$] contains orbits with $E \geq V_0$ [$E < V_0 - \delta_{\text{pb}}$] and $G_>$ coincides with G_{HK} (6). Accordingly, $G_>(t)$ describes the time evolution up to moderate times (comprising the parabolic range $V_0 - \delta_{\text{pb}}$ below the top) and $G_<(t)$ the long time behavior. Now, while in a strict sense the complex dynamics discussed above is only valid for very low E , we assume its applicability also for somewhat larger E and find with q_i and q_f on opposite sides of the barrier

$$G_<(q_f, q_i, t) = \int_{E < V_0 - \delta_{\text{pb}}} \frac{dqdp}{2\pi\hbar} h(q_f, q_i, t, p, q) R_<(p, q, t) e^{iS_<(p, q, t)/\hbar} T(q_0). \quad (8)$$

Here, an orbit runs from $\{p, q\}$ along the real axis to its TP $\{0, q_0\}$, jumps to $\{0, -q_0\}$ to reach $\{p(t), q(t)\}$ leading to a fluctuation prefactor $R_<$ and action $S_<$. The position space jump costs $T(q_0) = \exp[-|W(-q_0, q_0)|/\hbar]$ and eventually $G_<$ results from phase space averaging. In (8) we require $|q_i|/l, |q_f|/l \gg 1$ so that most of the dynamics is spent outside the barrier. Obviously, $G_<$ follows *not* just from switching in the integrand in $G_>$ to imaginary times in regions where $E < V(q)$.

IV. APPLICATIONS

The extended HK (eHK) $G_{\text{eHK}} = G_> + G_<$ is now employed to scattering in an Eckart barrier $V_b(q) = V_0/\cosh^2(q/l)$ that has been of wide use, e.g. as a model for the H+H₂ exchange reaction. Since asymptotically $V(q)$ drops faster than any power of q we have $\phi_c^+ \rightarrow 0$ and burning lines stretch parallel to the real axis. In fig. 2a the correlation function $c_{fi}(t) = \langle \psi_f | \exp(-iHt/\hbar) | \psi_i \rangle$ between two Gaussian wave packets is depicted. Initially, ψ_i [ψ_f] is centered to the far right [far left] with $V_0 \gg p_i^2/2$ so that we are indeed in a deep tunneling regime. One clearly sees the exponential drop of $G_>$ and the startling accuracy of the eHK over the whole time range. The most sensitive observable for a real-time treatment is the transmission probability $P(E)$ calculated by numerically Fourier transform $c_{fi}(t)$. Remarkably, we get accurate data also for very low energies (fig. 3) apart from small oscillations typical for real-time calculations [11]. In the moderate energy range $E/V_0 > 0.5$ the “real-time” $P(E)$ even improves the uniform WKB result. Here convergence for $G_<$ is achieved for roughly the same number of trajectories as in $G_>$ (typical number of trajectories for the set of parameters is $5 \cdot 10^4$) so that in contrast to previous approaches [10] an extension of the eHK to two or three dimensional systems, which are of particular interest to study

chaotic tunneling, seems feasible.

As an example where a dynamical approach is clearly needed we turn to an Eckart barrier driven by a periodic signal $V = V_b + qA \sin(\Omega t)$ and focus on the range of non-resonant driving and weak to moderate driving amplitudes. In this case already the exact numerics is non-trivial since it is the long time tunneling behavior which is most sensitively affected by the driving and leads to a strong spreading of the wave packet. Typical results for the correlation function $c_{fi}(t)$ are shown in fig. 2b. Compared to the static case one sees phase shifted oscillations and a revival type of phenomenon. Semiclassically, both effects originate from an intimate interference of (fast) above-barrier-paths ($E > V_0$), which cross the barrier and then are back-scattered, and (slow) driven tunneling orbits ($E < V_0$). Even in this time-dependent case the accuracy of the eHK is quite astonishing.

V. CONCLUSION

To conclude, our findings reveal for the first time how tunneling is encoded in the quantum propagator in terms of classical real-time orbits. In contrast to tunneling in the energy domain, real time barrier penetration cannot be described by individual tunneling orbits. Instead, it must be seen as a diffusion along a certain set of classical paths in the complex plane. This allows for a practical approach for semiclassical wave packet dynamics even in the deep tunneling regime of static and non-resonantly driven scattering processes. Explicit examples have been given for one dimensional cases, but the efficiency of the method suggests that at least two or three dimensional cases may be feasible. The main problem then will be that from a certain TP q_0 a bunch of TPs on the other side of the barrier can be reached. This proliferation of orbits, however, seems tractable due to the exponential suppression of under barrier motion starting at q_0 and traveling over large distances. Work in this direction is in progress. Possible applications of our method and extensions of it in physics and chemistry may be e.g. mesoscopic systems in microwave fields or unimolecular reactive scattering.

Financial support by the DFG through SFB276 is gratefully acknowledged.

[1] L.D. Landau, E.M. Lifshitz, *Quantum mechanics*, Pergamon, New York, 1965.

- [2] S.C. Creagh, N.D. Whelan, Phys. Rev. Lett. **77**, 4975 (1996).
- [3] M. Grifoni, P. Hänggi, Phys. Rep. **304**, 229 (1998).
- [4] O. Bohigas, S. Tomsovic, D. Ullmo, Phys. Rep. **223**, 43 (1993); A. Shudo and K.S. Ikeda, Phys. Rev. Lett. **74**, 682 (1995).
- [5] L.S. Schulman, *Techniques and Applications of Path Integration*, Wiley, New York, 1981.
- [6] M.F. Herman, E. Kluk, Chem. Phys. **91**, 27 (1984). F. Grossmann, A.L. Xavier, Phys. Lett. A **243**, 243 (1998).
- [7] S. Keshavamurthy, W.H. Miller, Chem. Phys. Lett. **218**, 189 (1994); N.T. Maitra, E.J. Heller, Phys. Rev. Lett. **78**, 3035 (1997); K.G. Kay, J. Chem. Phys. **107**, 2313 (1997).
- [8] F. Grossmann, E.J. Heller, Chem. Phys. Lett. **241**, 45 (1995).
- [9] V.A. Mandelshtam, M. Ovchinnikov, J. Chem. Phys. **108**, 9206 (1998).
- [10] F. Grossmann, Phys. Rev. Lett. **85**, 903 (2000).
- [11] S. Garashchuk, D.J. Tannor, Chem. Phys. Lett. **262**, 477 (1996).

FIG. 1: Orbits in the complex plane for $V_2(q) = 1/(1 + q^2)^2$ [thin; class (a) and (b) dotted, class (c) solid for various x_i and $\dot{y}_i > 0$, $\dot{y}_i < 0$]. Burning lines (thick) are shown for $V_2(q)$ (dashed) and its asymptote $1/q^4$ (solid); dots are TPs.

FIG. 2: Real part of c_{fl} vs. time for the static (a) and driven (b) scattering in an Eckart barrier. Parameters are $\gamma l^2 = 6$, $V_0/(p_i^2/2) = 8$, and (a) $q_i/l = -q_f/l = 40$, (b) $q_i/l = -q_f/l = 15$ with $q_i A/V_0 = -0.75$, $\Omega/\sqrt{V_0/2l^2} = 0.02$.

FIG. 3: Transmission probability vs. E/V_0 . Exact (solid), usual HK (dotted), eHK (dashed), and uniform WKB (dotted-dashed) are shown.

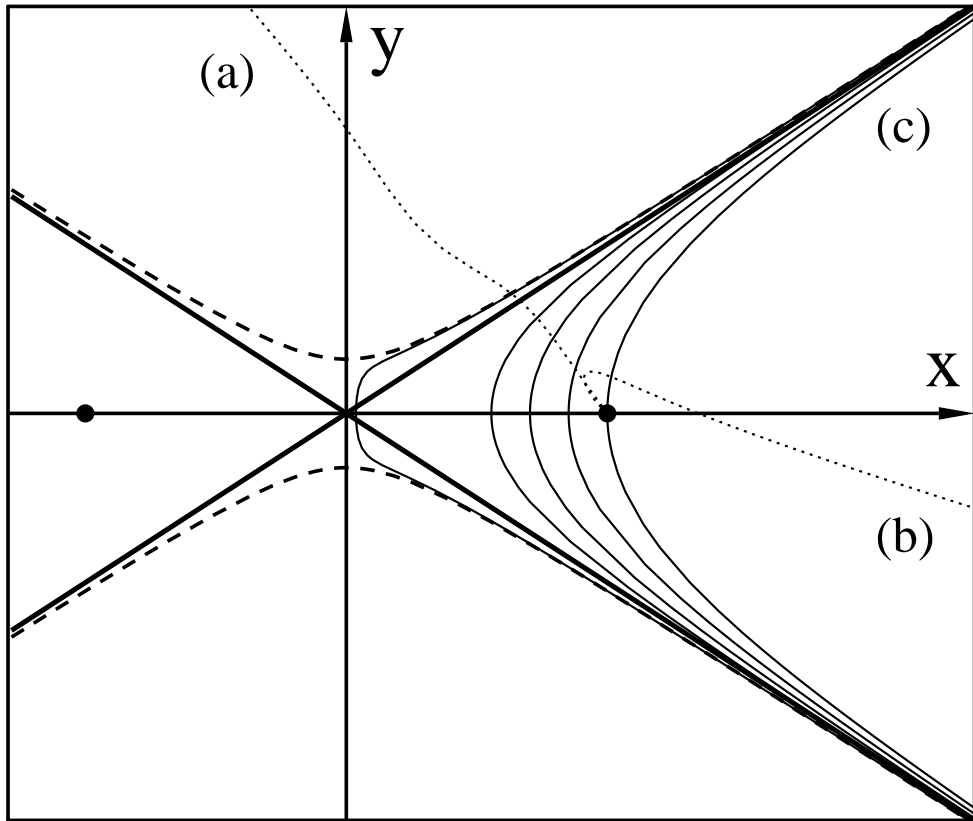
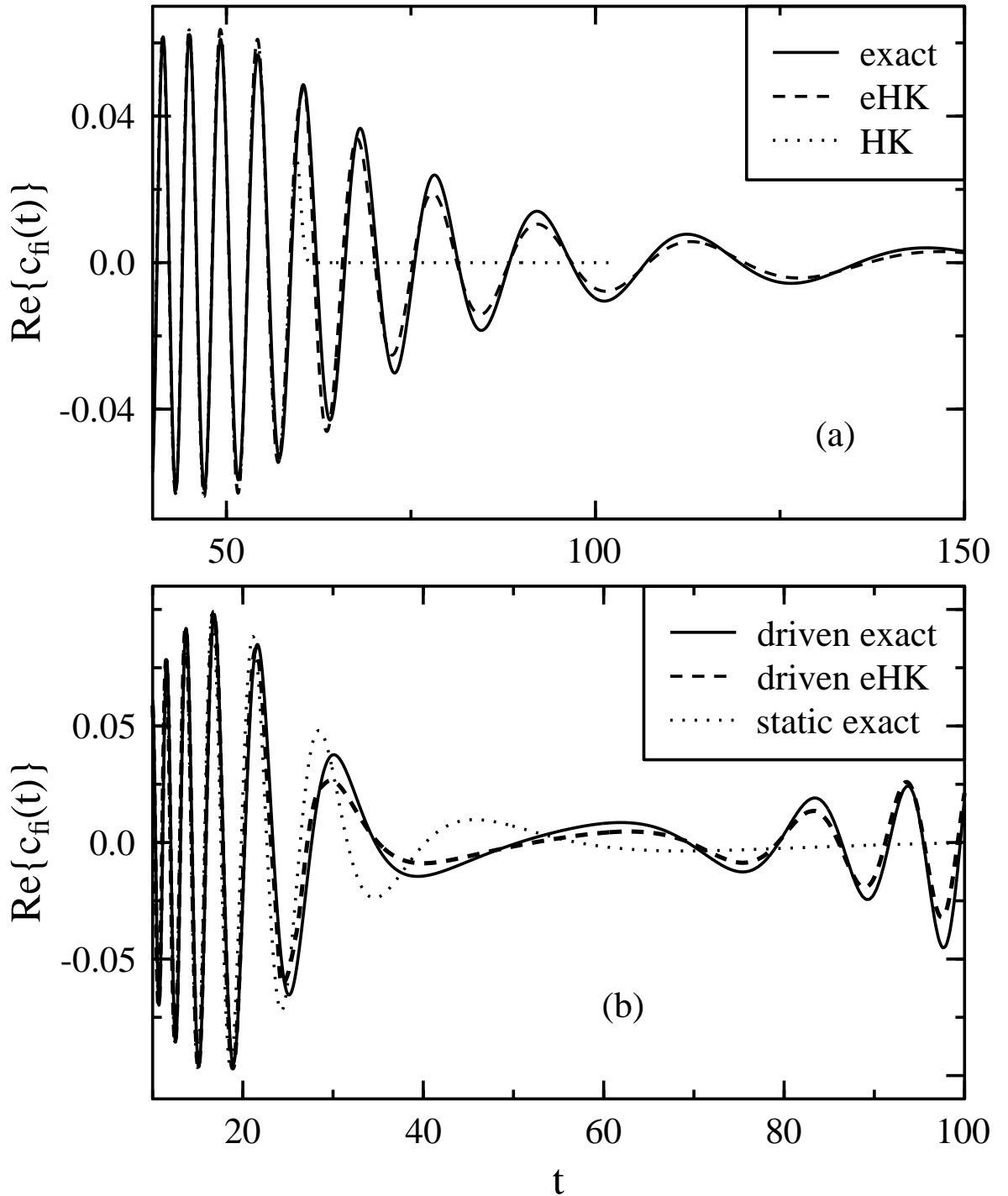


Figure 1: Ankerhold et al



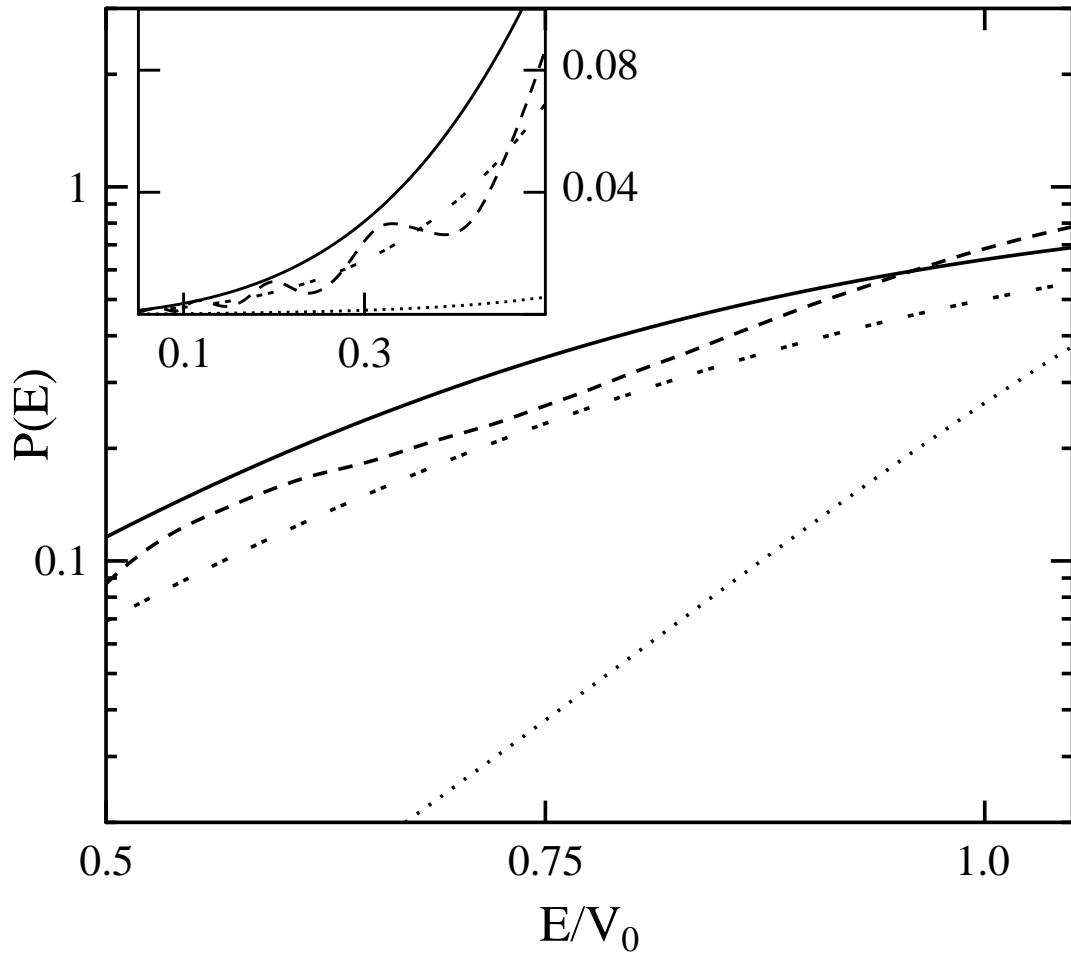


Figure 3: Ankerhold et al